Advances in Water Resources 68 (2014) 13–23

Contents lists available at ScienceDirect

Advances in Water Resources

journal homepage: www.elsevier.com/locate/advwatres

Analytical solutions for anomalous dispersion transport

D. O'Malley *, V.V. Vesselinov

Computational Earth Science Group, Earth and Environmental Sciences Division, Los Alamos National Laboratory, Los Alamos, NM, USA

ARTICLE INFO

Article history:
Received 1 October 2013
Received in revised form 19 February 2014
Accepted 20 February 2014
Available online 7 March 2014

Keywords:
Anomalous dispersion
Stochastic transport
Analytical solutions

ABSTRACT

Groundwater flow and transport often occur in a highly heterogeneous environment (potentially heterogeneous at multiple spatial scales) and is impacted by geochemical reactions, advection, diffusion, and other pore scale processes. All these factors can give rise to large-scale anomalous dispersive behavior that can make complex model representation and prediction of plume concentrations challenging due to difficulties unraveling all the complexities associated with the governing processes, flow medium, and their parameters. An alternative is to use upscaled stochastic models of anomalous dispersion, and this is the approach used here. Within a probabilistic framework, we derive a number of analytical solutions for several anomalous dispersion models. The anomalous dispersion models are allowed to be either non-Gaussian (α-stable Lévy), correlated, or nonstationary from the Lagrangian perspective. A global sensitivity analysis is performed to gain a greater understanding of the extent to which uncertainty in the parameters associated with the anomalous behavior can be narrowed by examining concentration measurements from a network of monitoring wells and to demonstrate the computational speed of the solutions. The developed analytical solutions are encoded and available for use in the open source computational framework MADS (http://mads.lanl.gov).

Published by Elsevier Ltd.

1. Introduction

Modeling groundwater transport presents a variety of significant theoretical and numerical challenges. One of these challenges is that anomalous dispersion is frequently observed in the field [e.g., 1,9,10,49,57]. There are a number of possible physical causes for anomalous behavior such as complex flowpaths caused by heterogeneities over a range of spatial scales (including fracture flow) [4,51], temporal variabilities in flow (due to, e.g., recharge events or pumping effects) [13,17,33], complex pore scale processes (due to, e.g., "dead end" pores, diffusion in low permeability zones or the solid matrix, etc.) [18,24,25,34,35], or complex biogeochemical interactions between liquid and solid species (e.g., sorption, redox reactions, etc.) [23,31,41].

One approach to modeling anomalous dispersion is to include more and more of the complex physics processes that cause the anomalous behavior. One might generate a sequence of hydraulic conductivity fields constrained by the conceptual understanding of rock formations in the environment and by measurements at a handful of locations to capture the heterogeneities. To capture the effect of recharge events, it may be necessary to use climate models coupled with groundwater flow models. An account of ever-increasing biogeochemical model complexity can be included as well. A modeler might proceed in this fashion and continue down the list adding more and more physics to the model. This is a worthwhile approach, but is not without drawbacks. These conglomerated models are usually not analytically tractable. Numerical models present difficulties for unraveling important correlations and interdependencies between model parameters and model predictions. Further, the characterization of the physical processes causing the anomalous diffusion behavior and identification of their impact on model predictions may be difficult, challenging, or impossible. Consequently, some aspects of the underlying physics may not make their way into even the most complex numerical model. Even with these limitations, the most complex models can be solved only on "stamp"-size domains with limited applicability for solving field-scale problems.

As a result, currently the applicability of complex models representing anomalous dispersion behavior for site studies is limited. However, anomalous dispersion behavior is commonly observed at actual sites [e.g., 5,48], often manifested in the form of scale-dependent dispersion [26,39]. This behavior can be critical for prediction of contaminant plume fate and designing potential remediation strategies. That is why the development of relatively simple mathematical models that can be applied in practice for model-based analyses such as uncertainty quantification (UQ)

* Corresponding author. Tel.: +1 5056678684.
E-mail addresses: omalled@lanl.gov (D. O'Malley), vvv@lanl.gov (V.V. Vesselinov).

http://dx.doi.org/10.1016/j.advwatres.2014.02.006
0309-1708/Published by Elsevier Ltd.

and capable of simulating anomalous dispersion behavior is important. The analytical solutions presented here represent a large range of the possible complexities associated with large-scale contaminant migration in an aquifer caused by different physical processes. Of course, this is by no means an exhaustive list of the many anomalous dispersion models presently used in subsurface hydrology. However, a general framework is derived where solutions can be presented for alternative models of anomalous dispersion using their probability, probability density, and cumulative distribution functions. These relatively simple analytical models can be calibrated against existing field observations of plume concentrations, and after that uncertainties in the model predictions can be quantified with more complex models being included in the uncertainty analysis without the need to solve them explicitly [43].

Alternative approaches used to represent anomalous dispersion behavior in large scale contaminant migration involve solving PDE's with fractional spatial [6,7] and/or temporal derivatives [40], continuous-time random walk techniques [8,40], or other particle-tracking methods [50,59]. The analytical approach used here is more in the spirit of these approaches. The advantage of the approach used here is that the spatial integrals can be solved analytically rather than numerically. The analytical approach has advantages for model analyses in relatively simple site settings. However, numerical approaches are preferred in cases when complex flow conditions need to be accounted for (e.g., pumping wells, recharge transients, etc.).

Mathematically, anomalous behavior is caused in the Lagrangian perspective by either heavy-tailed increments, correlated increments, or nonstationary increments [45]. An upscaled stochastic, dispersive process can be associated with each of these properties. Upscaled models provide a natural simplification of the complex underlying physics when the long-term behavior of the plume is the primary concern. The approach used here is to employ these stochastic models to derive analytical concentration functions while accounting for source type (e.g., point, areal, spatial, instantaneous, continious, etc.), initial conditions, boundary conditions (e.g., zero-flux or infinite), and contaminant degradation (biogeochemical reactions or radioactive decay). The speed of the analytical approach makes it possible to do forward modeling, parameter inversion, UQ, and sensitivity analyses as implemented in the current version of the MADS code [61,63]. Robust model analyses such as UQ often require more model runs ($>10^6$) than are possible with typical complex models and computational budgets. This is the application that motivates the development of these models.

The remainder of this manuscript is organized as follows. Section 2 covers the pertinent properties of the anomalous dispersive processes for which analytical solutions will be presented. Section 3 presents a derivation of the analytical form for the concentration where an arbitrary stochastic process is used for the dispersion. Section 4 uses this form to determine the concentration for specific stochastic processes and source types on an infinite and half-infinite domain with reflecting (zero-flux) boundary condition. Section 5 discusses a sensitivity analysis carried out using the analytical solutions that are developed in Section 4. Section 6 summarizes the results obtained.

2. Anomalous dispersion processes

A standard Brownian motion, $B(t)$, is defined analytically via three properties:

P1. The distribution of $B(t) - B(0)$ is Gaussian with zero mean and variance t.

P2. $B(t_1) - B(s_1)$ is independent from $B(t_2) - B(s_2)$ when there is no overlap between the intervals (t_1, s_1) and (t_2, s_2). That is, the displacements are independent.

P3. $B(t_1) - B(s_1)$ and $B(t_2) - B(s_2)$ have the same distribution when $t_1 - s_1 = t_2 - s_2$. That is, the displacements are identically distributed or stationary.

Brownian motion is the Lagrangian underpinning of classical/Fickian dispersion. Anomalous dispersive processes arise when one or more of these properties does not hold. There is a great variety of anomalous dispersive processes that result from relaxing these assumptions in different ways and in different combinations. Three examples will be considered here that arise from relaxing each one of the properties separately.

2.1. α-Stable Lévy motion

The property P1 makes sense in the context of dispersion because of the central limit theorem. A contaminant particle or parcel of fluid carrying contaminants moves by making a sequence of spatial displacements $[L]$, $X(n\Delta t) = \sum_{i=1}^{n} X(i\Delta t) - X([i-1]\Delta t)$ at given time increments Δt $[T]$. If $X(i\Delta t) - X([i-1]\Delta t)$ has finite variance is independent from and identically distributed to $X(j\Delta t) - X([j-1]\Delta t)$ whenever $i \neq j$, then the familiar central limit theorem implies that as n becomes large, $X(t)$ can be well-approximated by a Gaussian distribution. The assumptions of independent and identical distributions are closely related to the properties P2 and P3, respectively.

It is also true that the assumption of finite variance is closely related to the assumption P1. If there is no assumption of finite variance, a larger class of central limit distributions are produced. These distributions are called α-stable Lévy distributions [53,69,70], and have been used extensively to model hydrogeologic dispersion [cf. 6,7,55,56]. The parameter α can vary between 0 (exclusive) and 2 (inclusive). When $\alpha = 2$ the distribution is Gaussian. When $\alpha < 2$, the distributions can be skewed, tend to have more mass concentrated near the center (sharp peaks), and have "fat" or "heavy" tails whereas Gaussians tend to concentrate mass at an intermediate range. In the setting of subsurface transport the tail trailing behind the peak concentrations can be useful for capturing the effect of contaminants or fluid parcels that are stuck in a low conductivity zone. The tails ahead of the peak can be useful for capturing the effect of contaminants or fluid parcels moving through fractures or high conductivity channels. Lévy motions and their fractional Fokker–Planck equations have been presented as one explanation for the anomalous behavior at the MADE site [4].

A variety of parameterizations of the α-stable Lévy distributions are in use with the most common being the notation of [53], which we adopt here. In addition to the parameter α, there are three other distribution parameters. The parameter β $(-1 \leqslant \beta \leqslant 1)$ controls the skewness with positive beta producing a skew ahead of the peak and negative beta producing a skew behind the peak. The parameter γ is called the scale parameter. The parameter δ is called the shift parameter, because by modifying this parameter, the peak location is shifted. An α-stable random variable with these parameters is denoted $S_\alpha(\gamma, \beta, \delta)$.

One of the disadvantages of using α-stable Lévy distributions is that, unlike the Gaussian case, their probability density functions and cumulative density functions cannot be written in terms of simple, well-known functions like exponentials and square roots. However, in many special cases, they can be written in terms of "special" functions [28,32,37,47,54,71], and, in general, they can be written in terms of integrals that can only be solved numerically [42]. Software for computing these integrals is available [36]. Their functional forms are not going to be presented here; they can be

found in [42]. The probability density function of $S_\alpha(\gamma,\beta,\delta)$ will be denoted $f(x;\alpha,\gamma,\beta,\delta)$, and the cumulative density function will be denoted $F(x;\alpha,\gamma,\beta,\delta)$.

An α-stable Lévy motion is produced when properties P2 and P3 hold, but "Gaussian" in P1 is replaced with "α-stable Lévy." For the present purposes, it is necessary to know the probability density and cumulative density functions for a Lévy motion, $L(t)$. These are given by $f_L(x;\alpha,\gamma t^{1/\alpha},\beta,\delta)$ and $F_L(x;\alpha,\gamma t^{1/\alpha},\beta,\delta)$, respectively. The stability parameter, α, and the skewness parameter, β remain fixed in time. The scale parameter, γ, grows proportionally to $t^{1/\alpha}$. The shift parameter, δ, will be fixed constant throughout, because the shifting will be represented here through a drift term by replacing x with $x-vt$, where v is the advective (linear) flow velocity of contaminant migration and t is time since the migration started. For brevity, $a(t)$ will be used in place of the parameter list $(\alpha,\gamma t^{1/\alpha},\beta,\delta)$, so, e.g., $f_L(x;\alpha,\gamma t^{1/\alpha},\beta,\delta)$ can be written as $f_L(x;a(t))$.

2.2. Fractional Brownian motion

There are many ways to relax the property P2, but the most common and best studied approach is that of fractional Brownian motion [38]. For fractional Brownian motion, P2 does not hold, while P1 and P3 do hold. A fractional Brownian motion is usually denoted $B_H(t)$ where the parameter $0<H<1$ is called the Hurst exponent [–]. The distribution of $B_H(t)$ is normal with mean 0 and variance $\sigma^2 t^{2H}$ where σ is the scale parameter. When $H=1/2$, fractional Brownian motion is the same as Brownian motion. When $H\neq 1/2$, fractional Brownian motion is non-Markovian (*i.e.*, the probability distribution of future positions depends not only on the current position, but on the history of the process as well). When $H>1/2$, it is called persistent, meaning that once $B_H(t)$ starts to move in one direction, it tends to continue moving in that direction. This produces superdispersive behavior. When $H<1/2$, it is called anti-persistent, meaning that once $B_H(t)$ starts to move in one direction, it tends to double-back and move in the opposite direction. This produces subdispersive behavior. In a hydrogeological setting persistent velocity fluctuations may have a tendency to occur, especially in the longitudinal direction. For example, if the contaminant enters a low conductivity zone, it's velocity will tend to stay below the mean velocity for an extended period. Similarly, if the contaminant enters a high-velocity channel, its velocity may tend to stay above the mean velocity for an extended period. In contrast, anti-persistent velocity fluctuations may have a tendency to occur in transverse directions, perpendicular to the longitudinal flow.

With Hurst exponent H and scale parameter σ^2 $[L/T^H]$, the probability density function for a fractional Brownian motion is [38]

$$f_{FBM}(x,t;H,\sigma)=\frac{\exp\left(\frac{-x^2}{2\sigma^2 t^{2H}}\right)}{\sqrt{2\pi\sigma^2 t^{2H}}} \tag{1}$$

and the cumulative density function is

$$F_{FBM}(x,t;H,\sigma)=\frac{1}{2}\left[1+\operatorname{erf}\left(\frac{x}{\sqrt{2\sigma^2 t^{2H}}}\right)\right] \tag{2}$$

As before, drift can be imbued on fractional Brownian motion by replacing x with $x-vt$ in these functions.

2.3. Brownian motion with a nonlinear clock

Property P3 can be relaxed by the introduction of a nonlinear clock [14,15,44]. While P3 does not hold, P1 and P2 do hold. A Brownian motion with a nonlinear clock is given by $B(\mathfrak{C}(t;t_0))$ where $\mathfrak{C}(t;t_0)$ is a deterministic function called the clock, t_0 is the initial time (the time that the contaminant is injected into the aquifer). If $\mathfrak{C}(t;t_0)$ is not a linear function, the increments of $B(\mathfrak{C}(t;t_0))$ are not stationary, and P3 does not hold. The clock should be expressible in the form

$$\mathfrak{C}(t;t_0)=\int_{t_0}^{t}\frac{\partial\mathfrak{C}(s;t_0)}{\partial s}ds \tag{3}$$

where $\frac{\partial\mathfrak{C}(t;t_0)}{\partial t}\geqslant 0$. We call the clock Lagrangian if it depends only on $t-t_0$. If $\frac{\partial\mathfrak{C}(t;t_0)}{\partial t}$ depends only on t, it is called Eulerian. Consider two examples to illustrate the utility of these different styles of clocks. A Lagrangian clock may be appropriate in an advection dominated regime in a heterogeneous media that evolves in *space*, specifically in the direction of flow. In this case, the dispersive properties of the medium at different locations would be embedded in the clock, since the time can be used to approximate the position in an advection dominated regime ($X(t)\approx x_0+v_x(t-t_0)$,$Y(t)\approx y_0+v_y(t-t_0)$, $Z(t)\approx z_0+v_z(t-t_0)$). This approach will work best when the dispersivities are smooth functions so that approximating the dispersivity at $(X(t),Y(t),Z(t))$ with the dispersivity at $(x_0+v_x(t-t_0)$, $y_0+v_y(t-t_0),z_0+v_z(t-t_0))$ will not cause significant errors. An Eulerian clock may be appropriate if contaminants are dispersing in a homogeneous medium that is evolving in *time*, for example, due to changes in pore structure due to mineral deposition or dissolution. In this case, the changes of the dispersive properties of the medium at different times would be embedded in the clock. The form for the clock in Eq. (3) and the assumption that $\frac{\partial\mathfrak{C}(t;t_0)}{\partial t}$ does not depend on t_0 implies that for a contaminant injected at time t_0, the clock will only depend on the properties of the medium beginning at time t_0.

The functional form and parameters of the clock subordinator in both the Lagrangian and Eulerian flavor implicitly depend on flow characteristics. Inverse estimation of $\mathfrak{C}(t;t_0)$ based on observed concentration $c(\mathbf{x},t)$ or trajectory data for a tracer or fluid parcels can be challenging because there are so many possibilities (any increasing function of t suffices). If many Lagrangian trajectories are available, it can be estimated from the quadratic variation [16] (cf.[3], for an example where this is practical). Another alternative is to derive an appropriate clock from the properties of the porous medium, but given limited knowledge for most contamination sites, this may be challenging as well.

For many practical cases, a simplification of the functional form of the possible clocks may be necessary assuming a power (e.g., $\mathfrak{C}(t;t_0)=\sigma^2 t^p$), exponential (e.g., $\mathfrak{C}(t;t_0)=\sigma^2\exp(pt)$), or periodic (e.g., $\mathfrak{C}(t;t_0)=\sigma^2\sin(pt)$) functional forms (where σ and p are unknown parameters; for the Lagrangian case, t needs to replaced with $t-t_0$). These three forms represent a power law, exponential and periodic changes in the dispersion properties. These three functional forms can be also combined to represent coupled mechanisms.

The probability density function for Brownian motion with a nonlinear clock is [14]

$$f_{NLC}(x,t;\mathfrak{C}(t;t_0))=\frac{\exp\left(\frac{-x^2}{2\mathfrak{C}(t;t_0)}\right)}{\sqrt{2\pi\mathfrak{C}(t;t_0)}} \tag{4}$$

and the cumulative density function is

$$F_{NLC}(x,t;\mathfrak{C}(t;t_0))=\frac{1}{2}\left[1+\operatorname{erf}\left(\frac{x}{\sqrt{2\mathfrak{C}(t;t_0)}}\right)\right] \tag{5}$$

Once again, drift can be imbued on this process by replacing x in Eqs. (5) and (4) with $x-vt$ and $x-v(t-t_0)$ in the Eulerian and Lagrangian case, respectively.

2.4. Other anomalous processes

Three processes have been examined by relaxing each of the properties P1, P2, and P3 separately. It is, of course, possible to

relax two or three of these properties simultaneously producing, e.g., fractional Brownian motion with a nonlinear clock [44], α-stable Lévy motion with a nonlinear clock, fractional Lévy motions [53], or fractional Lévy motion with a nonlinear clock. Another possibility is to replace the deterministic clocks by random subordinators [2]. In determining the analytical solutions, we will proceed by deriving the general case for an arbitrary dispersive process, and then considering the three special cases of anomalous dispersion discussed in Sections 2.1–2.3. If analytical solutions are required for anomalous processes other than these three, the work required to determine a new analytical solution will be to determine the probability density function or cumulative density function (depending on the type of source) and to plug it into the general case.

3. Probabilistic derivation

Suppose that contaminant is introduced into an aquifer over time with an injection rate $Q(\mathbf{x},t)$ $[M/L^3]$, has a constant advective (linear) velocity $\mathbf{v}=(v,0,0)$ $[L/T]$ oriented in the x-direction, undergoing mass reduction from biochemical reactions or radioactive decay, and the dispersion of a particle is determined by random walks $\mathbf{P}(t)=(X(t),Y(t),Z(t))$. For Fickian dispersion, these random walks would be Brownian motions with potentially different dispersion coefficients. In general, the processes may not be Fickian, and the random walks may not be Brownian motions. That is, the displacements may be correlated in time, non-stationary, or non-Gaussian as discussed above.

The goal is to determine analytical expressions for the concentration of contaminants that are moving in this way. First, some notation must be introduced. Let $f_{\mathbf{P}}(\mathbf{x},t), f_X(x,t), f_Y(y,t)$ and $f_Z(z,t)$ denote the probability density functions for the random walks $\mathbf{P}(t), X(t), Y(t)$, and $Z(t)$. The probability density function at time t for such a particle that is released at $\mathbf{x}_0$ at time t_0 is $f_{\mathbf{P}}(\mathbf{x}-\mathbf{v}(t-t_0)-\mathbf{x}_0, t-t_0; t_0)$ owing to the effects of advection (represented by the $\mathbf{v}t$ term) and dispersion (represented by the use of $f_{\mathbf{P}}$).

The contaminant is injected at a rate $Q(\mathbf{x},t)$ can be interpreted probabilistically, where $Q(\mathbf{x},t)/m(t)$ is the probability density function for contaminant particles or parcels, and

$$m(t)=\int_{\mathbb{R}^3} Q(\mathbf{x},t)d\mathbf{x} \tag{6}$$

is the mass flux $[M/T]$ at time t. Assuming that the initial condition is independent of the random walk, the probability density function for an instantaneous release of a contaminant particle at time $t-\tau$ is

$$\int_{\mathbb{R}^3} \frac{Q(\mathbf{y},t-\tau) f_{\mathbf{P}}(\mathbf{x}-\mathbf{y}-\mathbf{v}\tau,\tau;t-\tau)}{m(t-\tau)} d\mathbf{y} \tag{7}$$

Eq. (7) follows from the fact that the probability density function of two independent random variables is given by the convolution of their respective probability density functions.

Accounting for the reduction in mass, the differential concentration at time t for contaminants injected at time $t-\tau$ over an infinitesimal time interval, $d\tau$, is

$$dC(\mathbf{x},t)=R(\tau,t-\tau)\int_{\mathbb{R}^3} Q(\mathbf{y},t-\tau) f_{\mathbf{P}}(\mathbf{x}-\mathbf{y}-\mathbf{v}\tau,\tau;t-\tau)d\mathbf{y}d\tau \tag{8}$$

where $R(\tau,t)$ is the fraction of the contaminant mass released at time t that remains after time $t+\tau$. For example, if a first-order reaction is taking place with a rate λ $[1/T]$,

$$R(\tau,t-\tau)=e^{-\lambda\tau} \tag{9}$$

Alternative formulations of $R(\tau,t-\tau)$ can be used to incorporate more complex reaction models. For example, some of the effects of incomplete mixing at scales smaller than the field scale can be incorporated using mean concentration functions form, cf., [11] which have late-time power laws. This approach assumes that the averaged concentrations in [11] can be regarded as field-scale concentrations for our purposes, and that the mixing is incomplete at the pore or meso scales. Several methods for incorporating chemical reactions into particle tracking methods also have recently been developed [11,12,20–22,46,67,68]. Generally, these approaches require significant computational effort (compared to the solutions presented here) and are not analytically tractable. Analytical solutions for reactive transport can be derived in some cases [19,29], but it is not clear how to extend these approaches to a general anomalous dispersion process. Here, it is not assumed that the field-scale dispersion that we explore determines the processes impacting contaminant degradation at the pore and meso scales; we only consider the field-scale degradation as presented Eq. (8). This decoupling of the dispersion and degradation at the field scale is an approximation. However, simulations and experiments at pore, meso and field scales can be performed to inform the site-specific selection of $R(\tau,t)$. $R(\tau,t)$ provides a means to account for the pore- and meso-scale dispersion (flow) affects on the field-scale degradation (concentrations), and $\mathfrak{C}(t;t_0)$ provides a means to account for the pore- and meso-scale biogeochemical affects on the field-scale dispersion within the nonlinear clock formulation. Therefore we provide implicit coupling of these processes. Simulations and experiments at pore, meso and field scales can be performed to inform the site-specific selection of $\mathfrak{C}(t;t_0)$

Finally, integrating Eq. (8) over time, we obtain the contaminant concentration following the description given in the first paragraph of Section 3,

$$C(\mathbf{x},t)=\int_0^t\int_{\mathbb{R}^3} R(\tau,t-\tau)Q(\mathbf{y},t-\tau)\, f_{\mathbf{P}}(\mathbf{x}-\mathbf{y}-\mathbf{v}\tau,\tau)d\mathbf{y}d\tau \tag{10}$$

Note that Eq. (10) is a more general form of the many solutions given in [65,66]. By making additional assumptions on injection concentration, $Q(\mathbf{x},t)$, and the random walks through $f_{\mathbf{P}}(\mathbf{x},t)$, the solutions can be made more explicit. To demonstrate this, several cases will be considered.

4. Special cases

We now present a series of special cases of Eq. (10). The first consists of a contaminant released uniformly inside a finite domain represented by a set B over a finite time interval (t_1,t_2). The solution for an arbitrary anomalous dispersive process is included as are specific solutions for the three anomalous processes discussed in Section 2.

4.1. Constrained source

Suppose that the release of the contaminant is constrained temporally inside the time interval (t_1,t_2) and spatially inside the set B. This is written mathematically

$$Q^c(\mathbf{x},t)=\begin{cases}\frac{M\chi_{(t_1,t_2)}(t)}{n||B||(t_2-t_1)}, & \mathbf{x}\in B \text{ and } t_1<t<t_2\\ 0, & \text{otherwise}\end{cases}$$

where

$$\chi_{(t_1,t_2)}(t)=\begin{cases}1, & \text{if } t\in(t_1,t_2)\\ 0, & \text{if } t\notin(t_1,t_2)\end{cases} \tag{11}$$

M is the contaminant mass $[M]$, n is the porosity $[-]$, and $||B||$ is the volume in which the source is contained $[L^3]$. In this case, the concentrations can be written in terms of the cumulative density function rather than an integral of the probability density function

$$C(\mathbf{x},t) = \int_0^t \int_B R(\tau, t-\tau)\frac{M}{n||B||(t_2-t_1)}\chi_{(t_1,t_2)}(t-\tau) \times f_{\mathbf{P}}(\mathbf{x}-\mathbf{y}-\mathbf{v}\tau,\tau;t-\tau)d\mathbf{y}dt \quad (12)$$

$$= \frac{M}{n||B||(t_2-t_1)}\int_0^t \chi_{(t_1,t_2)}(t-\tau)R(\tau,t-\tau) \times \int_B f_{\mathbf{P}}(\mathbf{x}-\mathbf{y}-\mathbf{v}\tau,\tau;t-\tau)d\mathbf{y}dt \quad (13)$$

$$= \frac{M}{n||B||(t_2-t_1)}\int_0^t \chi_{(t_1,t_2)}(t-\tau)R(\tau,t-\tau) \times P(\mathbf{P}(\tau;t-\tau)\in \mathbf{x}-B-\mathbf{v}\tau)dt \quad (14)$$

where $P(\mathbf{P}(\tau;t)\in A)$ is the probability of finding a particle that was released at time t in the set A at time $t+\tau$.

If it is further assumed that the dispersions along each coordinate axis are unrelated so that $X(t), Y(t)$, and $Z(t)$ are independent and B is a box bounded by the intervals $(x_1,x_2),(y_1,y_2)$, and (z_1,z_2), then

$$C(\mathbf{x},t) = \frac{M}{n||B||(t_2-t_1)}\int_0^t \chi_{(t_1,t_2)}(t-\tau)R(\tau,t-\tau) \times \{[F_X(x-x_1-v\tau,\tau;t-\tau)-F_X(x-x_2-v\tau,\tau;t-\tau)] \times [F_Y(y-y_1,\tau;t-\tau)-F_Y(y-y_2,\tau;t-\tau)] \times [F_Z(z-z_1,\tau;t-\tau)-F_Z(z-z_2,\tau;t-\tau)]\}d\tau \quad (15)$$

where $F_X(x,t;\tau), F_Y(y,t;\tau)$, and $F_Z(z,t;\tau)$ are the cumulative density functions for $X(t), Y(t)$ and $Z(t)$ with initial times τ.

4.1.1. Dispersion via α-stable Lévy motion

Inserting the cumulative density function for α-stable Lévy motion into Eq. (14), we obtain

$$C(\mathbf{x},t) = \frac{M}{n||B||(t_2-t_1)}\int_0^t \chi_{(t_1,t_2)}(t-\tau)R(\tau,t-\tau) \times \{[F_X(x-x_1-v\tau,\tau;t-\tau)-F_X(x-x_2-v\tau,\tau;t-\tau)] \times [F_Y(y-y_1,\tau;t-\tau)-F_Y(y-y_2,\tau;t-\tau)] \times [F_Z(z-z_1,\tau;t-\tau)-F_Z(z-z_2,\tau;t-\tau)]\}d\tau \quad (16)$$

where $a_x(\tau)=\alpha_x,\gamma_x t^{1/\alpha_x},\beta_x,\delta_x$ (similarly for $a_y(\tau)$ and $a_z(\tau)$) and different parameters α,β,γ, and δ are allowed in each of the coordinate directions. Figs. 1 and 2 display example concentrations for a plume based on Brownian motion (classical Fickian dispersion) and α-stable Lévy motion. The model setup and parameters are discussed in Section 5 below. A comparison of the figures demonstrate the pronounced impact of the motion type on the plume shape and contaminant concentrations. As expected the α-stable Lévy motion (Fig. 2) produced "heavy" tails of contaminant concentrations at the plume leading edges, whereas Brownian motion tended to concentrate contaminant mass near the source (Fig. 1).

4.1.2. Dispersion via fractional Brownian motion

Inserting Eq. (2) into Eq. (15) and simplifying, we obtain

$$C(\mathbf{x},t) = \frac{M}{8n||B||(t_2-t_1)}\int_0^t \chi_{(t_1,t_2)}(t-\tau)R(\tau,t-\tau) \times \left\{\left[\mathrm{erf}\left(\frac{x-x_1-v\tau}{\sqrt{2\sigma_x^2\tau^{H_x}}}\right)-\mathrm{erf}\left(\frac{x-x_2-v\tau}{\sqrt{2\sigma_x^2\tau^{H_x}}}\right)\right] \times \left[\mathrm{erf}\left(\frac{y-y_1}{\sqrt{2\sigma_y^2\tau^{H_y}}}\right)-\mathrm{erf}\left(\frac{y-y_2}{\sqrt{2\sigma_y^2\tau^{H_y}}}\right)\right] \times \left[\mathrm{erf}\left(\frac{z-z_1}{\sqrt{2\sigma_z^2\tau^{H_z}}}\right)-\mathrm{erf}\left(\frac{z-z_2}{\sqrt{2\sigma_z^2\tau^{H_z}}}\right)\right]\right\}d\tau \quad (17)$$

where different parameters H and σ are permitted in each of the coordinate directions. Figs. 3 and 4 display the concentrations for a plume based on Eq. (17) (Section 5 below discusses the model setup and parameters). Note the substantial differences in the plume shapes between the superdispersive and subdispersive cases. In this case, the spatial distribution of predicted concentrations for superdispersive (Fig. 3) and α-stable Lévy motion (Fig. 2) are similar in the pictured spatial region. The subdispersive case retain the contaminants close to the source; if these data were interpreted with Brownian motion, they may be considered indicative of low transport velocity and/or large contaminant source area. Note also that behaviors such as superdispersion in the longitudinal direction and subdispersion in the lateral directions can be modeled by setting $H_x > 1/2$ and $H_y, H_z < 1/2$.

4.1.3. Dispersion via Brownian motion with a nonlinear clock

Inserting Eq. (5) into Eq. (15) and simplifying, we obtain

$$C(\mathbf{x},t) = \frac{M}{8n||B||(t_2-t_1)}\int_0^t \chi_{(t_1,t_2)}(t-\tau)R(\tau,t-\tau) \times \left\{\left[\mathrm{erf}\left(\frac{x-x_1-v\tau}{\sqrt{2\mathfrak{C}_x(\tau;t-\tau)}}\right)-\mathrm{erf}\left(\frac{x-x_2-v\tau}{\sqrt{2\mathfrak{C}_x(\tau;t-\tau)}}\right)\right] \times \left[\mathrm{erf}\left(\frac{y-y_1}{\sqrt{2\mathfrak{C}_y(\tau;t-\tau)}}\right)-\mathrm{erf}\left(\frac{y-y_2}{\sqrt{2\mathfrak{C}_y(\tau;t-\tau)}}\right)\right] \times \left[\mathrm{erf}\left(\frac{z-z_1}{\sqrt{2\mathfrak{C}_z(\tau;t-\tau)}}\right)-\mathrm{erf}\left(\frac{z-z_2}{\sqrt{2\mathfrak{C}_z(\tau;t-\tau)}}\right)\right]\right\}d\tau \quad (18)$$

where different clocks are permitted in each of the coordinate directions. Figs. 5 and 6 display the concentrations for a plume

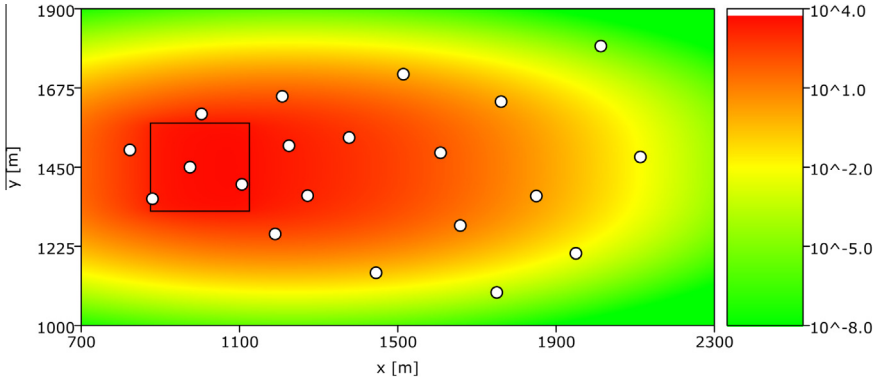

Fig. 1. Plume with box source that is dispersing via Brownian motion ($v_x = 5$ [m/a], concentrations in mg/m^3).

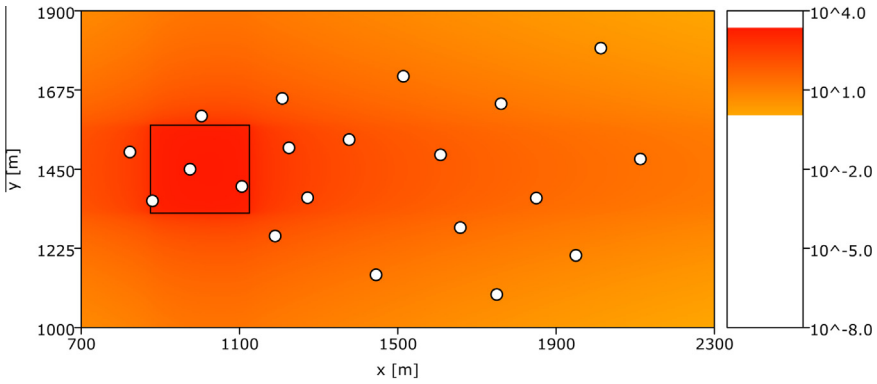

Fig. 2. Plume with box source that is dispersing via Lévy motion ($v_x = 5$ [m/a], $\alpha = 1.1$, concentrations in mg/m^3).

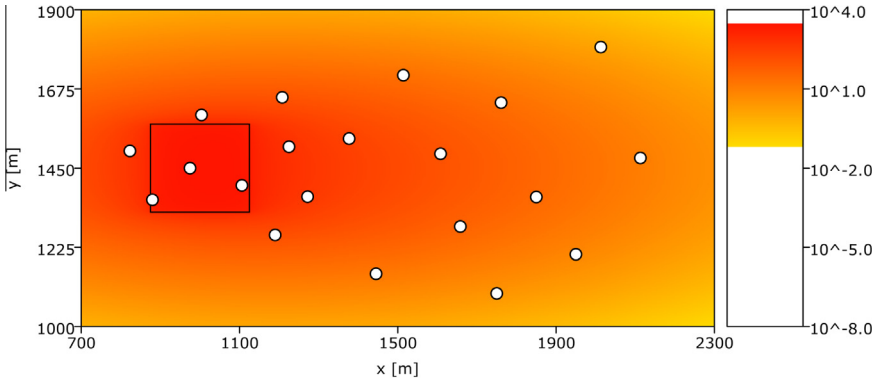

Fig. 3. Plume with box source that is dispersing via a superdispersive (persistent) fractional Brownian motion ($v_x = 5$ [m/a], $H = 3/4$, concentrations in mg/m^3).

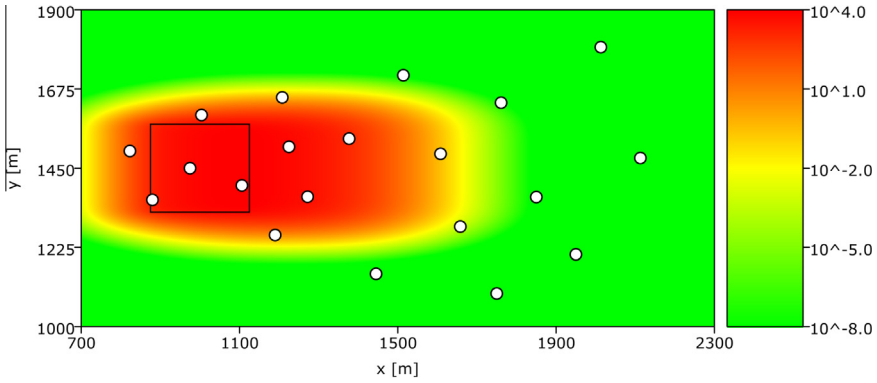

Fig. 4. Plume with box source that is dispersing via a subdispersive (anti-persistent) fractional Brownian motion ($v_x = 5$ [m/a], $H = 1/4$, concentrations in mg/m^3).

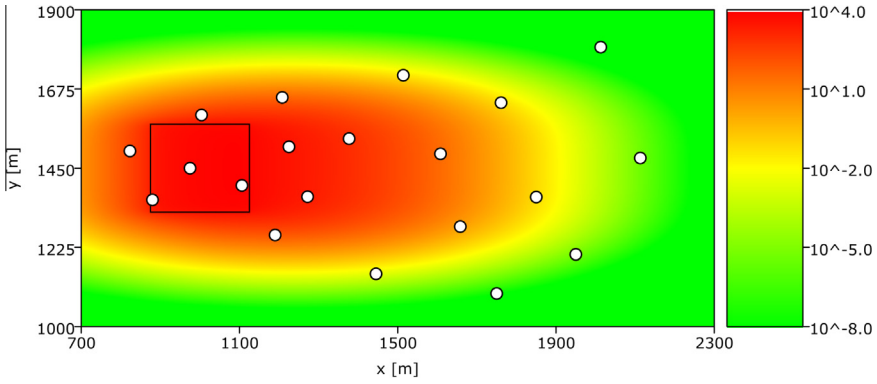

Fig. 5. Plume with box source that is dispersing via Brownian motion with a nonlinear clock that is initially accelerating ($v_x = 5$ [m/a], $\mathfrak{C}(t) = t - 50\sin(t/100)$, concentrations in mg/m^3).

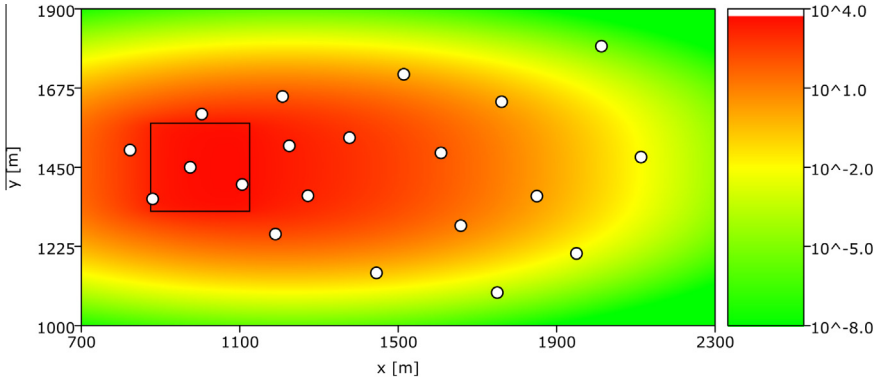

Fig. 6. Plume with box source that is dispersing via Brownian motion with a nonlinear clock that is initially decelerating ($v_x = 5$ [m/a], $\mathfrak{C}(t) = t + 50\sin(t/100)$, concentrations in mg/m^3).

based on Eq. (18). The two figures represent two different Lagrangian clock models. In the first case (Fig. 5), the dispersion is initially accelerated and after that it is slowed down with time; in the second case, (Fig. 6) this mechanism was reversed.

4.2. Constrained source with reflecting boundary

Suppose that a semi-infinite space with a reflecting boundary (zero flux) at $z = 0$ is used in place of the infinite three-dimensional space used previously. Applying the method of images to Eq. (14), the new concentration is obtained

$$\begin{aligned} C(\mathbf{x},t) = {} & \frac{M}{n||B||(t_2-t_1)} \int_0^t \chi_{(t_1,t_2)}(t-\tau) R(\tau, t-\tau) \\ & \times [P(\mathbf{P}(t;t-\tau) \in (x,y,z) - B - \mathbf{v}\tau) \\ & + P(\mathbf{P}(t;t-\tau) \in (x,y,-z) - B - \mathbf{v}\tau)] dt \end{aligned} \tag{19}$$

where $\mathbf{P}(t)$ is the original, non-reflected process.

Proceeding as before, if it is assumed that the dispersions along each coordinate axis are unrelated so that $X(t), Y(t)$, and $Z(t)$ are independent and B is a box bounded by the intervals $(x_1, x_2), (y_1, y_2)$, and (z_1, z_2), then

$$\begin{aligned} C(\mathbf{x},t) = {} & \frac{M}{n||B||(t_2-t_1)} \int_0^t \chi_{(t_1,t_2)}(t-\tau) R(\tau, t-\tau) \\ & \times \{[F_X(x - x_1 - v\tau, \tau; t-\tau) - F_X(x - x_2 - v\tau, \tau; t-\tau)] \\ & \times [F_Y(y - y_1, \tau; t-\tau) - F_Y(y - y_2, \tau; t-\tau)] \\ & \times [F_Z(z - z_1, \tau; t-\tau) - F_Z(z - z_2, \tau; t-\tau) \\ & + F_Z(-z - z_1, \tau; t-\tau) - F_Z(-z - z_2, \tau; t-\tau)]\} d\tau \end{aligned} \tag{20}$$

where $F_X(x,t;\tau), F_Y(y,t;\tau)$, and $F_Z(z,t;\tau)$ are the cumulative density functions for $X(t), Y(t)$ and $Z(t)$ with initial times τ.

4.2.1. Dispersion via α-stable Lévy motion

Inserting the cumulative density function for α-stable Lévy motion into Eq. (14), we obtain

$$\begin{aligned} C(\mathbf{x},t) = {} & \frac{M}{n||B||(t_2-t_1)} \int_0^t \chi_{(t_1,t_2)}(t-\tau) R(\tau, t-\tau) \\ & \times \{[F_L(x - x_1 - v\tau; a_x(\tau)) - F_L(x - x_2 - v\tau; a_x(\tau))] \\ & \times [F_L(y - y_1; a_y(\tau)) - F_L(y - y_2; a_y(\tau)] \\ & \times [F_L(z - z_1; a_z(\tau)) - F_L(z - z_2; a_z(\tau)) \\ & + F_L(-z - z_1; a_z(\tau)) - F_L(-z - z_2; a_z(\tau))]\} d\tau \end{aligned} \tag{21}$$

where $a_x(\tau) = \alpha_x, \gamma_x t^{1/\alpha_x}, \beta_x, \delta_x$ (similarly for $a_y(\tau)$ and $a_z(\tau)$) and different parameters α, β, γ, and δ are allowed in each of the coordinate directions.

4.2.2. Dispersion via fractional Brownian motion

Inserting Eq. (2) into Eq. (15) and simplifying, we obtain

$$\begin{aligned} C(\mathbf{x},t) = {} & \frac{M}{8n||B||(t_2-t_1)} \int_0^t \chi_{(t_1,t_2)}(t-\tau) R(\tau, t-\tau) \\ & \times \left\{ \left[\operatorname{erf}\left(\frac{x - x_1 - v\tau}{\sqrt{2\sigma_x^2 \tau^{H_x}}} \right) - \operatorname{erf}\left(\frac{x - x_2 - v\tau}{\sqrt{2\sigma_x^2 \tau^{H_x}}} \right) \right] \right. \\ & \times \left[\operatorname{erf}\left(\frac{y - y_1}{\sqrt{2\sigma_y^2 \tau^{H_y}}} \right) - \operatorname{erf}\left(\frac{y - y_2}{\sqrt{2\sigma_y^2 \tau^{H_y}}} \right) \right] \\ & \times \left[\operatorname{erf}\left(\frac{z - z_1}{\sqrt{2\sigma_z^2 \tau^{H_z}}} \right) - \operatorname{erf}\left(\frac{z - z_2}{\sqrt{2\sigma_z^2 \tau^{H_z}}} \right) \right. \\ & \left. \left. + \operatorname{erf}\left(\frac{-z - z_1}{\sqrt{2\sigma_z^2 \tau^{H_z}}} \right) - \operatorname{erf}\left(\frac{-z - z_2}{\sqrt{2\sigma_z^2 \tau^{H_z}}} \right) \right] \right\} d\tau \end{aligned} \tag{22}$$

where different parameters H and σ are permitted in each of the coordinate directions.

4.2.3. Dispersion via Brownian motion with a nonlinear clock

Inserting Eq. (5) into Eq. (15) and simplifying, we obtain

$$\begin{aligned} C(\mathbf{x},t) = {} & \frac{M}{8n||B||(t_2-t_1)} \int_0^t \chi_{(t_1,t_2)}(t-\tau) R(\tau, t-\tau) \\ & \times \left\{ \left[\operatorname{erf}\left(\frac{x - x_1 - v\tau}{\sqrt{2\mathfrak{C}_x(\tau; t-\tau)}} \right) - \operatorname{erf}\left(\frac{x - x_2 - v\tau}{\sqrt{2\mathfrak{C}_x(\tau; t-\tau)}} \right) \right] \right. \\ & \times \left[\operatorname{erf}\left(\frac{y - y_1}{\sqrt{2\mathfrak{C}_y(\tau; t-\tau)}} \right) - \operatorname{erf}\left(\frac{y - y_2}{\sqrt{2\mathfrak{C}_y(\tau; t-\tau)}} \right) \right] \\ & \times \left[\operatorname{erf}\left(\frac{z - z_1}{\sqrt{2\mathfrak{C}_z(\tau; t-\tau)}} \right) - \operatorname{erf}\left(\frac{z - z_2}{\sqrt{2\mathfrak{C}_z(\tau; t-\tau)}} \right) \right. \\ & \left. \left. + \operatorname{erf}\left(\frac{-z - z_1}{\sqrt{2\mathfrak{C}_z(\tau; t-\tau)}} \right) - \operatorname{erf}\left(\frac{-z - z_2}{\sqrt{2\mathfrak{C}_z(\tau; t-\tau)}} \right) \right] \right\} d\tau \end{aligned} \tag{23}$$

where different clocks are permitted in each of the coordinate directions.

4.3. Distributed sources

We next consider a number of cases where the contaminant is preexisting in the aquifer in some dispersed state and the future concentrations are estimated using the presented analytical solutions for anomalous dispersion. The way that the contaminant is initially distributed is assumed to be related to the dispersion model. For the two anomalous Gaussian models (fractional Brownian motion and Brownian motion with a nonlinear clock),

the initial distribution is Gaussian. For α-stable Lévy motion, the initial distribution is α-stable.

4.4. Dispersion via α-stable Lévy motion

We now consider α-stable Lévy motion as the model for dispersion with a source that also follows an independent α-stable distribution in each of the coordinate directions with a time-dependent mass flux. The mathematical formulation for this source is given by

$$Q^l(\mathbf{x},t) = \frac{M f_L(x;a_x^0) f_L(y;a_y^0) f_L(z;a_z^0) I(t)}{n} \tag{24}$$

where $\int_0^\infty I(t)dt = 1, M$ is the total contaminant mass added to the aquifer, n is the porosity, and $a_x^0 = (\alpha_x, \gamma_x^0, \beta_x^0, \delta_x^0)$ are the parameters associated with the α-stable Lévy distributions in the x direction (similarly for a_y^0 and a_z^0). If Eq. (24) is placed in Eq. (10) with

$$f_{\mathbf{P}}(\mathbf{x},t) = f_L(x - vt; a_x(t)) f_L(y; a_y(t)) f_L(z; a_z(t)) \tag{25}$$

where $a_x(t) = (\alpha_x, \gamma_x t^{1/\alpha_x}, \beta_x, 0)$ (and similarly for $a_y(t)$ and $a_z(t)$) then each of the integrals along the spatial coordinates is a convolution of two Lévy stable distributions with the same stability parameter. This convolution can be interpreted as the distribution for the sum of two independent Lévy stable distributions. The distribution of the sum of two independent α-stable Lévy distributions is another α-stable Lévy distribution. If the parameters of the two α-stable distributions are $\alpha, \gamma_1, \beta_1, \delta_1$ and $\alpha, \gamma_2, \beta_2, \delta_2$ then the distribution of their sum is α-stable with parameters [53]

$$\gamma = (\gamma_1^\alpha + \gamma_2^\alpha)^{1/\alpha} \tag{26}$$

$$\beta = \frac{\beta_1 \gamma_1^\alpha + \beta_2 \gamma_2^\alpha}{\gamma_1^\alpha + \gamma_2^\alpha} \tag{27}$$

$$\delta = \delta_1 + \delta_2 \tag{28}$$

Therefore, the concentration can be written as

$$C(\mathbf{x},t) = \frac{M}{n} \int_0^t R(t-\tau,\tau) I(\tau) f_L(x - v(t-\tau); a_x'(t-\tau)) \times f_L(y; a_y'(t-\tau)) f_L(z; a_z'(t-\tau)) dt d\tau \tag{29}$$

where $a_x'(t) = \left(\alpha_x, ([\gamma_x^0]^\alpha + \gamma_x^\alpha t)^{1/\alpha}, \frac{\beta_x^0 [\gamma_x^0]^\alpha + \beta_x \gamma_x^\alpha t}{[\gamma_x^0]^\alpha + \gamma_x^\alpha t}, \delta_x^0\right)$, and similarly for $a_y'(t)$ and $a_z'(t)$.

4.5. Dispersion via fractional Brownian motion

Next we consider fractional Brownian dispersion with a Gaussian source and a time-dependent mass flux. The functional form for this source is

$$Q^g(\mathbf{x},t) = \frac{M I(t)}{n \sigma_x^0 \sigma_y^0 \sigma_z^0 \sqrt{8\pi^3}} exp\left(-\frac{(x-\mu_x^0)^2}{2[\sigma_x^0]^2} - \frac{(y-\mu_y^0)^2}{2[\sigma_y^0]^2} - \frac{(z-\mu_z^0)^2}{2[\sigma_z^0]^2} \right) \tag{30}$$

If Eq. (30) is placed in Eq. (10) with

$$f_{\mathbf{P}}(\mathbf{x},t) = f_{FBM}(x - vt, t; H_x, \sigma_x) f_{FBM}(y, t; H_y, \sigma_y) f_{FBM}(z, t; H_z, \sigma_z) \tag{31}$$

the result is

$$C(\mathbf{x},t) = \frac{M}{n} \int_0^t R(t-\tau,\tau) I(\tau) \times \frac{exp\left(-\frac{(x-\mu_x - v(t-\tau))^2}{2([\sigma_x^0]^2 + \sigma_x^2 (t-\tau)^{2H})} - \frac{(y-\mu_y)^2}{2([\sigma_y^0]^2 + \sigma_y^2 (t-\tau)^{2H})} - \frac{(z-\mu_z)^2}{2([\sigma_z^0]^2 + \sigma_z^2 (t-\tau)^{2H})} \right)}{\sqrt{8\pi^3 \left([\sigma_x^0]^2 + \sigma_x^2 (t-\tau)^{2H}\right)\left([\sigma_y^0]^2 + \sigma_y^2 (t-\tau)^{2H}\right)\left([\sigma_z^0]^2 + \sigma_z^2 (t-\tau)^{2H}\right)}} d\tau \tag{32}$$

where the same derivation that was previously implemented for the convolution of two α-stable distributions was reproduced here for the convolution of two Gaussians.

4.6. Dispersion via Brownian motion with a nonlinear clock

The computation of the concentration for dispersion via Brownian with a nonlinear clock and a Gaussian source is essentially the same as the derivation when the dispersion is follows a fractional Brownian motion. The concentration in this case is

$$C(\mathbf{x},t) = \frac{M}{n} \int_0^t R(t-\tau,\tau) I(\tau) \times \frac{exp\left(-\frac{(x-\mu_x - v(t-\tau))^2}{2([\sigma_x^0]^2 + \mathfrak{C}_x(t-\tau;\tau))} - \frac{(y-\mu_y)^2}{2([\sigma_y^0]^2 + \mathfrak{C}_y(t-\tau;\tau))} - \frac{(z-\mu_z)^2}{2([\sigma_z^0]^2 + \mathfrak{C}_z(t-\tau;\tau))} \right)}{\sqrt{8\pi^3 \left([\sigma_x^0]^2 + \mathfrak{C}_x(t-\tau;\tau)\right)\left([\sigma_y^0]^2 + \mathfrak{C}_y(t-\tau;\tau)\right)\left([\sigma_z^0]^2 + \mathfrak{C}_z(t-\tau;\tau)\right)}} d\tau \tag{33}$$

5. Sensitivity analysis

A global sensitivity analysis based on Sobol's method [58] was performed for each of the anomalous models presented above as well as for Brownian motion (classical Fickian dispersion model). In order to compute the sensitivity, first the model was used to produce nominal concentrations at a number of wells at a number of times ranging from 0 [a] to 50 [a] for each of the models. The plumes are generated by a 3D source with a straight parallelepiped (box) shape centered at (x,y,z) = (1000, 1450, 0) [m] and with dimensions (dx,dy,dz) = (250, 250, 1) [m]. The contaminant source is located at the top of an aquifer with infinite extent. The constant mass flux is 16 [kg/a]. The plume shapes for $t = 50$ [a] are presented in Figs. 1–6 for different models (model parameters are listed in the figure captions); the concentrations are shown in mg/m^3. The spatial distribution of the observation wells is presented in the same figures as white circles. The objective function used in the sensitivity analyses was the sum of the squared differences between the nominal concentrations and the concentrations produced by the model with parameters differing from the nominal case. In all cases, the sensitivity was taken with respect to the velocity, dispersion coefficients, and first order reaction rate. All the parameters were assumed to be distributed uniformly. The pore (linear) velocity v varied from 4 [m/a] to 6 [m/a] with a nominal value of 5 [m/a]. The x dispersivity, a_x, varied from 10 [m] to 140 [m] with a nominal value of 70 [m], and the y and z dispersivities were tied to this and smaller by a factor of 10 and 50, respectively. The dispersion coefficient, D_x, was va_x, and similarly for D_y and D_z. It is assumed that the reaction is first-order, so Eq. (9) is obeyed and λ ranged from 0 to 0.01 [1/a]. The aquifer porosity is equal to 0.1.

For Lévy motion, the sensitivity was also taken with respect to α which varied from 1.1 (the value observed at the MADE site [4]) to 2 (the classical Gaussian value) with a nominal value of 1.5. In the Lévy motion case, the skewness parameter, β, was fixed at 0, so the distributions were symmetric. The scale parameters (γ_x, γ_y, and γ_z) were given by $D_x^{1/\alpha}, D_y^{1/\alpha}, D_z^{1/\alpha}$, respectively. For fractional Brownian motion, the sensitivity was also taken with respect to the Hurst exponent, H, and two cases were considered. One was a superdispersive case with H ranging from 0.5 to 1.0 with a nominal value of $H = 0.75$. The other was a subdispersive case with H ranging from 0.05 to 0.5 with a nominal value of 0.25. In both cases, the parameters σ_x^2, σ_y^2, and σ_z^2 were taken to be equal to D_x, D_y, and D_z, respectively. For Brownian motion with a non-linear clock, two clocks were considered, $\mathfrak{C}_{x,1}(t;t_0) = D_x[t + 100a\sin(t/100)]$ and $\mathfrak{C}_{x,2}(t;t_0) = D_x[t - 100a\sin(t/100)]$, with a ranging from 0 [a] to 1 [a] with a nominal value of 0.5 [a] in both cases. The clocks for

Table 1
The first order sensitivities of parameters for several dispersion models.

First Order	v	D_x	λ	α	H	a
BM	0.03	0.95	0.01	N/A	N/A	N/A
Lévy	0.01	0.40	0.00	0.30	N/A	N/A
FBM, $H \geq 0.5$	0.01	0.39	0.00	N/A	0.32	N/A
FBM, $H \leq 0.5$	0.02	0.34	0.02	N/A	0.26	N/A
BM-NLC, $\mathfrak{C}_1(t)$	0.02	0.35	0.00	N/A	N/A	0.54
BM-NLC, $\mathfrak{C}_2(t)$	0.00	0.14	0.00	N/A	N/A	0.48

Table 2
The total effect of parameters for several dispersion models.

Total Effect	v	D_x	λ	α	H	a
BM	0.05	0.97	0.01	N/A	N/A	N/A
Lévy	0.03	0.68	0.00	0.58	N/A	N/A
FBM, $H \geq 0.5$	0.03	0.66	0.00	N/A	0.60	N/A
FBM, $H \leq 0.5$	0.04	0.71	0.02	N/A	0.63	N/A
BM-NLC, $\mathfrak{C}_1(t)$	0.02	0.43	0.01	N/A	N/A	0.66
BM-NLC, $\mathfrak{C}_2(t)$	0.03	0.51	0.01	N/A	N/A	0.85

the y and z coordinates are the same, except that D_x is replaced with D_y and D_z, respectively. In all cases, the appropriate form of Eq. (15) was used with $x_1 = 750$ [m], $x_2 = 1250$ [m], $y_1 = 1200$ [m], $y_2 = 1700$ [m], $z_1 = 0$ [m], $z_2 = 1$ [m], $t_1 = 0$ [a], and $t_2 = 100$ [a].

Each sensitivity analysis was performed using 1,000,000 samples using a double Latin hypercube approach [52]. The sensitivity analyses were performed using the open source computational framework MADS [63]. The results of the analyses are summarized in Tables 1 and 2, giving the first-order sensitivity and total effect, respectively (in Saltelli's terminology [52]). Generally, the plume behavior is much more sensitive to the dispersion coefficient than the velocity, partially due to the fact that the dispersion coefficient varied over a large range compared to the velocity. The sensitivity to the reaction rate, λ, is very small. This could change if a greater uncertainty range were considered. The main point of interest is the sensitivity to the parameters characterizing the anomalous behavior. For the case of Lévy motion, the concentrations are highly sensitive to the value of α with the sensitivity coefficients being comparable to the sensitivity of the dispersion coefficient. In the case of fractional Brownian motion, the results are similar to the Lévy case with a strong sensitivity to the anomalous dispersion parameter (H in this case). The plume concentrations are relatively insensitive to the a parameter in the clocks. It should be noted, however, that a different choice of clocks could potentially produce high sensitivities. For example, if the clock were a power-law with coefficient equal to the dispersion coefficient, the sensitivities would be the same as the fractional Brownian motion sensitivities (if the range of powers in the power law is taken to be the same as twice the range of the Hurst exponent). The general conclusion that can be reached from this analysis is that plume concentrations can be highly sensitive to the parameters associated with anomalous behavior, especially in the case of the parameter α (which controls the tail behavior) in the case of Lévy motion. We also note that for each model, 1,000,000 runs were performed each characterizing field scale dispersion over a 50 year time period. Tests show that this is the order of magnitude of the number of runs needed to produce reliable sensitivity estimates for these problems. Similar or greater demands are expected from other UQ methods. This demonstrates the power of the analytical solutions over alternative numerical methods for contaminant simulations.

6. Conclusion

A number of analytical functions describing the concentration of subsurface contaminant migration undergoing advection, chemical reactions, and anomalous dispersion have been derived. Three different anomalous dispersion processes were considered representing upscaled, macroscopic approximations that can be associated with different flow medium properties and governing physical processes. The use of α-stable Lévy distributions has previously been associated with highly heterogeneous hydraulic conductivity fields [4]. The fractional Brownian model of dispersion arises when there are long range correlations between the velocity fluctuations [60] caused by, e.g., long range correlations in hydraulic conductivity combined with a relatively constant hydraulic gradient. The nonlinear clock model arises when the distribution of the velocity fluctuations is changing in time caused by, e.g., pumping effects, seasonal fluctuations, or evolving pore-space structure (due to, for example, mineral dissolution or precipitation) [16]. This is not meant to be an exhaustive list of anomalous processes or the underlying physics that cause them. Each of the considered anomalous processes moves one step beyond the standard Gaussian dispersion model, allowing for the possibility of more complex underlying physics to be accounted for. The sensitivity analyses performed as well as the figures demonstrate that these anomalous parameters can have a significant impact on the distribution of the plume.

A significant advantage of these analytical solutions is that, when implemented on a computer, they are fast compared to complex numerical codes. They are complex in comparison to the Gaussian dispersion model, and the computational demands are comparable (though interpolation routines may be necessary in the α-stable case). Therefore, they exist in a middle ground. They are not able to capture all of the details of the complex numerical models, but they capture more of the details than the Gaussian dispersion model. The fact that the computational cost is similar to the Gaussian model implies that many model analyses that are possible with the Gaussian model are also possible with these anomalous models. For example, methods such as [27,62] for parameter estimation, [30,64] for uncertainty analysis, and [43] for decision analyses are readily applicable in practice. The analytical solutions presented here are encoded in the open source computational framework MADS [63].

Acknowledgments

The authors wish to thank four anonymous reviewers for comments that substantially improved the manuscript. This research was funded by the Environmental Programs Directorate of the Los Alamos National Laboratory; the Advanced Simulation Capability for Environmental Management (ASCEM) project, Department of Energy, Environmental Management; and the Integrated Multifaceted Approach to Mathematics at the Interfaces of Data, Models, and Decisions (DiaMonD) project, Department of Energy, Office of Science.

References

[1] Eric Adams E, Gelhar Lynn W. Field study of dispersion in a heterogeneous aquifer: 2. spatial moments analysis. Water Resour Res 1992;28(12):3293–307. http://dx.doi.org/10.1029/92WR01757.
[2] Baeumer Boris, Benson David A, Meerschaert Mark M, Wheatcraft Stephen W. Subordinated advection-dispersion equation for contaminant transport. Water Resour Res 2001;37(6):1543–50. http://dx.doi.org/10.1029/2000WR900409.
[3] Bassler Kevin E, McCauley Joseph L, Gunaratne Gemunu H. Nonstationary increments, scaling distributions, and variable diffusion processes in financial markets. Proc Natl Acad Sci 2007;104(44):17287–90. http://dx.doi.org/10.1073/pnas.0708664104.
[4] Benson David A, Schumer Rina, Meerschaert Mark M, Wheatcraft Stephen W. Fractional dispersion, Lévy motion, and the made tracer tests. Transp Porous Media 2001;42(1–2):211–40. http://dx.doi.org/10.1023/A:1006733002131.
[5] Benson David A, Schumer Rina, Meerschaert Mark M, Wheatcraft Stephen W. Fractional dispersion, lévy motion, and the made tracer tests. In: Dispersion in heterogeneous geological formations. Springer; 2002. p. 211–40.
[6] Benson David A, Wheatcraft Stephen W, Meerschaert Mark M. Application of a fractional advection–dispersion equation. Water Resour Res 2000;36(6):1403–12. http://dx.doi.org/10.1029/2000WR900031.

[7] Benson David A, Wheatcraft Stephen W, Meerschaert Mark M. The fractional-order governing equation of Lévy motion. Water Resour Res 2000;36(6):1413–23. http://dx.doi.org/10.1029/2000WR900032.
[8] Berkowitz Brian, Cortis Andrea, Dentz Marco, Scher Harvey. Modeling non-fickian transport in geological formations as a continuous time random walk. Rev Geophys 2006;44(2). http://dx.doi.org/10.1029/2005RG000178.
[9] Mark Boggs J, Eric Adams E. Field study of dispersion in a heterogeneous aquifer: 4. investigation of adsorption and sampling bias. Water Resour Res 1992;28(12):3325–36. http://dx.doi.org/10.1029/92WR01759.
[10] Mark Boggs J, Young Steven C, Beard Lisa M, Gelhar Lynn W, Rehfeldt Kenneth R, Eric Adams E. Field study of dispersion in a heterogeneous aquifer: 1. overview and site description. Water Resour Res 1992;28(12):3281–91. http://dx.doi.org/10.1029/92WR01756.
[11] Bolster Diogo, de Anna Pietro, Benson David A, Tartakovsky Alexandre M. Incomplete mixing and reactions with fractional dispersion. Adv Water Resour 2012;37:86–93. http://dx.doi.org/10.1016/j.advwatres.2011.11.005.
[12] Choi TaiJung, Maurya Mano Ram, Tartakovsky Daniel M, Subramaniam Shankar. Stochastic operator-splitting method for reaction–diffusion systems. J Chem Phys 2012;137(18). http://dx.doi.org/10.1063/1.4764108. 184102–184102.
[13] Cortis Andrea, Knudby Christen. A continuous time random walk approach to transient flow in heterogeneous porous media. Water Resour Res 2006;42(10). http://dx.doi.org/10.1029/2006WR005227.
[14] Cushman John H, O'Malley Daniel, Park Moongyu. Anomalous diffusion as modeled by a nonstationary extension of Brownian motion. Phys Rev E 2009;79(3):032101. http://dx.doi.org/10.1103/PhysRevLett.112.068103.
[15] Cushman John H, Park Moongyu, O'Malley Daniel. Chaotic dynamics of super-diffusion revisited. Geophys Res Lett 2009;36(8). http://dx.doi.org/10.1029/2009GL037399.
[16] Cushman John H, Park Moongyu, O'Malley Daniel. A stochastic model for anomalous diffusion in confined nano-films near a strain-induced critical point. Adv Water Resour 2011;34(4):490–4. http://dx.doi.org/10.1016/j.advwatres.2011.01.005.
[17] Dagan G. Analysis of flow through heterogeneous random aquifers: 2. unsteady flow in confined formations. Water Resour Res 1982;18(5):1571–85. http://dx.doi.org/10.1029/WR018i005p01571.
[18] Dagan G, Fiori A, Janković I. Flow and transport in highly heterogeneous formations: 1. conceptual framework and validity of first-order approximations. Water Resour Res 2003;39(9):1268. http://dx.doi.org/10.1029/2002WR001717.
[19] De Simoni M, Carrera J, Sanchez-Vila X, Guadagnini A. A procedure for the solution of multicomponent reactive transport problems. Water Resour Res 2005;41(11):W11410. http://dx.doi.org/10.1029/2005WR004056.
[20] Ding Dong, Benson David A, Paster Amir, Bolster Diogo. Modeling bimolecular reactions and transport in porous media via particle tracking. Adv Water Resour 2012;53:56–65. http://dx.doi.org/10.1016/j.advwatres.2012.11.001.
[21] Edery Yaniv, Scher Harvey, Berkowitz Brian. Modeling bimolecular reactions and transport in porous media. Geophys Res Lett 2009;36(2):L02407. http://dx.doi.org/10.1029/2008GL036381.
[22] Edery Yaniv, Scher Harvey, Berkowitz Brian. Particle tracking model of bimolecular reactive transport in porous media. Water Resour Res 2010;46(7). http://dx.doi.org/10.1029/2009WR009017.
[23] Erin Feehley C, Zheng Chunmiao, Molz Fred J. A dual-domain mass transfer approach for modeling solute transport in heterogeneous aquifers: Application to the macrodispersion experiment (made) site. Water Resour Res 2000;36(9):2501–15. http://dx.doi.org/10.1029/2000WR900148.
[24] Fiori A, Janković I, Dagan G. Flow and transport in highly heterogeneous formations: 2. semianalytical results for isotropic media. Water Resour Res 2003;39(9):1269. http://dx.doi.org/10.1029/2002WR001719.
[25] Fiori A, Janković I, Dagan G. Modeling flow and transport in highly heterogeneous three-dimensional aquifers: ergodicity, gaussianity, and anomalous behavior-2. Approximate semianalytical solution. Water Resour Res 2006;42(6):W06D13. http://dx.doi.org/10.1029/2005WR004752.
[26] Gelhar Lynn W, Welty Claire, Rehfeldt Kenneth R. A critical review of data on field-scale dispersion in aquifers. Water Resour Res 1992;28(7):1955–74. http://dx.doi.org/10.1029/92WR00607.
[27] Kashif Gill M, Kaheil Yasir H, Khalil Abedalrazq, McKee Mac, Bastidas Luis. Multiobjective particle swarm optimization for parameter estimation in hydrology. Water Resour Res 2006;42(7). http://dx.doi.org/10.1029/2005WR004528.
[28] Górska K, Penson KA. Lévy stable two-sided distributions: exact and explicit densities for asymmetric case. Phys Rev E 2011;83(6):061125. http://dx.doi.org/10.1103/PhysRevE.83.061125.
[29] Gramling Carolyn M, Harvey Charles F, Meigs Lucy C. Reactive transport in porous media: a comparison of model prediction with laboratory visualization. Environ Sci Technol 2002;36(11):2508–14. http://dx.doi.org/10.1021/es0157144.
[30] Harp Dylan R, Vesselinov Velimir V. An agent-based approach to global uncertainty and sensitivity analysis. Comput Geosci 2012;40:19–27. http://dx.doi.org/10.1016/j.cageo.2011.06.025.
[31] Harvey Charles, Gorelick Steven M. Rate-limited mass transfer or macrodispersion: which dominates plume evolution at the macrodispersion experiment (made) site? Water Resour Res 2000;36(3):637–50. http://dx.doi.org/10.1029/1999WR900247.
[32] Hoffmann-Jrgensen Jrgen. Stable densities. Theory Probab Appl 1993;38(2):350–5. http://dx.doi.org/10.1137/1138031.
[33] Indelman Peter. Averaging of unsteady flows in heterogeneous media of stationary conductivity. J Fluid Mech 1996;310:39–60. http://dx.doi.org/10.1017/S0022112096001723.
[34] Janković I, Fiori A, Dagan G. Flow and transport in highly heterogeneous formations: 3. numerical simulations and comparison with theoretical results. Water Resour Res 2003;39(9):1270. http://dx.doi.org/10.1029/2002WR001721.
[35] Janković I, Fiori A, Dagan G. Modeling flow and transport in highly heterogeneous three-dimensional aquifers: ergodicity, gaussianity, and anomalous behavior-1. conceptual issues and numerical simulations. Water Resour Res 2006;42(6). http://dx.doi.org/10.1029/2005WR004734.
[36] Liang Yingjie, Chen Wen. A survey on computing Lévy stable distributions and a new matlab toolbox. In: Signal processing; 2012. http://dx.doi.org/10.1016/j.sigpro.2012.07.035.
[37] Mainardi Francesco, Pagnini Gianni, Saxena RK. Fox h functions in fractional diffusion. J Comput Appl Math 2005;178(1):321–31. http://dx.doi.org/10.1016/j.cam.2004.08.006.
[38] Mandelbrot Benoit B, Van Ness John W. Fractional Brownian motions, fractional noises and applications. SIAM Rev 1968;10(4):422–37. http://dx.doi.org/10.1137/1010093.
[39] Martinez-Landa Lurdes, Carrera Jesús. An analysis of hydraulic conductivity scale effects in granite (full-scale engineered barrier experiment (febex), Grimsel, Switzerland). Water Resour Res 2005;41(3). http://dx.doi.org/10.1029/2004WR003458.
[40] Metzler Ralf, Klafter Joseph. The random walk's guide to anomalous diffusion: a fractional dynamics approach. Phys Rep 2000;339(1):1–77. http://dx.doi.org/10.1016/S0370-1573(00)00070-3.
[41] Molz Fred J, Zheng Chunmiao, Gorelick Steven M, Harvey Charles F. Comment on investigating the macrodispersion experiment (made) site in Columbus, Mississippi, using a three-dimensional inverse flow and transport model by Heidi Christiansen Barlebo, Mary C. Hill, and Dan Rosbjerg. Water Resour Res 2006;42(6). http://dx.doi.org/10.1029/2005WR004265.
[42] John Nolan P. Numerical calculation of stable densities and distribution functions. Commun Stat Stochastic Models 1997;13(4):759–74. http://dx.doi.org/10.1080/15326349708807450.
[43] O'Malley D, Vesselinov VV. Groundwater remediation using the information gap decision theory. Water Resour Res 2014;50:246–56. http://dx.doi.org/10.1002/2013WR014718.
[44] O'Malley Daniel, Cushman John H. Fractional Brownian motion run with a nonlinear clock. Phys Rev E 2010;82(3):032102. http://dx.doi.org/10.1103/PhysRevLett.112.068103.
[45] O'Malley Daniel, Cushman John H. Two-scale renormalization-group classification of diffusive processes. Phys Rev E 2012;86(1):011126. http://dx.doi.org/10.1103/PhysRevLett.112.068103.
[46] Paster A, Bolster D, Benson DA. Particle tracking and the diffusion-reaction equation. Water Resour Res 2013;49:1–6. http://dx.doi.org/10.1029/2012WR012444.
[47] Penson KA, Górska K. Exact and explicit probability densities for one-sided Lévy stable distributions. Phys Rev Lett 2010;105(21):210604. http://dx.doi.org/10.1103/PhysRevLett.105.210604.
[48] Pickens John F, Grisak Gerald E. Scale-dependent dispersion in a stratified granular aquifer. Water Resour Res 1981;17(4):1191–211. http://dx.doi.org/10.1029/WR017i004p01191.
[49] Rehfeldt Kenneth R, Mark Boggs J, Gelhar Lynn W. Field study of dispersion in a heterogeneous aquifer: 3. geostatistical analysis of hydraulic conductivity. Water Resour Res 1992;28(12):3309–24. http://dx.doi.org/10.1029/92WR01758.
[50] Robinson Bruce A, Dash Zora V, Srinivasan Gowri. A particle tracking transport method for the simulation of resident and flux-averaged concentration of solute plumes in groundwater models. Comput Geosci 2010;14(4):779–92. http://dx.doi.org/10.1007/s10596-010-9190-6.
[51] Salamon P, Fernàndez-Garcia D, Gómez-Hernández JJ. Modeling tracer transport at the made site: the importance of heterogeneity. Water Resour Res 2007;43(8):W08404. http://dx.doi.org/10.1029/2006WR005522.
[52] Saltelli Andrea. Making best use of model evaluations to compute sensitivity indices. Comput Phys Commun 2002;145(2):280–97. http://dx.doi.org/10.1016/S0010-4655(02)00280-1.
[53] Samorodnitsky G, Taqqu MS. Stable non-Gaussian random processes: stochastic models with infinite variance. New York: Chapman & Hall; 1994.
[54] Schneider WR. Stable distributions: Fox function representation and generalization. Springer; 1986.
[55] Schumer Rina, Benson David A, Meerschaert Mark M, Baeumer Boris. Fractal mobile/immobile solute transport. Water Resour Res 2003;39(10):1296. http://dx.doi.org/10.1029/2003WR002141.
[56] Schumer Rina, Benson David A, Meerschaert Mark M, Baeumer Boris. Multiscaling fractional advection–dispersion equations and their solutions. Water Resour Res 2003;39(1):1022. http://dx.doi.org/10.1029/2001WR001229.
[57] Sidle Roy C, Nilsson Bertel, Hansen Martin, Fredericia Johnny. Spatially varying hydraulic and solute transport characteristics of a fractured till determined by field tracer tests, Funen, Denmark. Water Resour Res 1998;34(10):2515–27. http://dx.doi.org/10.1029/98WR01735.
[58] Sobol Ilya M. Global sensitivity indices for nonlinear mathematical models and their Monte Carlo estimates. Math Comput Simul 2001;55(1–3):271–80. http://dx.doi.org/10.1016/S0378-4754(00)00270-6.

[59] Srinivasan G, Tartakovsky Daniel M, Dentz M, Viswanathan H, Berkowitz B, Robinson BA. Random walk particle tracking simulations of non-fickian transport in heterogeneous media. J Comput Phys 2010;229(11):4304–14. http://dx.doi.org/10.1016/j.jcp.2010.02.014.
[60] Taqqu Murad S. Fractional brownian motion and long-range dependence, in: Theory and Applications of Long-Range Dependence, 2003, pp. 5–38.
[61] Vesselinov Velimer V, Harp D. Model analysis and decision support (mads) for comple physics models. In: XIX International conference on water resources-CMWR; 2012.
[62] Vesselinov Velimir V, Harp Dylan R. Adaptive hybrid optimization strategy for calibration and parameter estimation of physical process models. Comput Geosci 2012;49:10–20. http://dx.doi.org/10.1016/j.cageo.2012.05.027.
[63] Vesselinov Velimir V, O'Malley Daniel, Harp Dylan. Model analysis and decision support (mads). In: XIX International conference on water resources-CMWR; 2013.
[64] Vrugt Jasper A, Ter Braak CJF, Diks CGH, Robinson Bruce A, Hyman James M, Higdon Dave. Accelerating Markov chain Monte Carlo simulation by differential evolution with self-adaptive randomized subspace sampling. Int J Nonlinear Sci Numer Simul 2009;10(3):273–90. http://dx.doi.org/10.1515/IJNSNS.2009.10.3.273.
[65] Wang Hongtao, Huayong Wu. Analytical solutions of three-dimensional contaminant transport in uniform flow field in porous media: a library. Frontiers Environ Sci Eng Chin 2009;3(1):112–28. http://dx.doi.org/10.1007/s11783-008-0067-z.
[66] Wexler Eliezer J. Analytical solutions for one-, two-, and three-dimensional solute transport in ground-water systems with uniform flow. US Geologic Survery; 1992. http://dx.doi.org/10.1103/PhysRevLett.112.068103.
[67] Zhang Yong, Papelis Charalambos. Particle-tracking simulation of fractional diffusion–reaction processes. Phys Rev E 2011;84(6):066704. http://dx.doi.org/10.1002/wrcr.20368.
[68] Zhang Yong, Papelis Charalambos, Sun Pengtao, Yu Zhongbo. Evaluation and linking of effective parameters in particle-based models and continuum models for mixing-limited bimolecular reactions. Water Resour Res 2013;49(8):4845–65. http://dx.doi.org/10.1002/wrcr.20368.
[69] Zolotarev VM. One-dimensional stable distributions, vol. 65. American Mathematical Society; 1986.
[70] Zolotarev Vladimir M. Modern theory of summation of random variables. Walter de Gruyter; 1997.
[71] Zolotarev Vladimir Mikhailovich. On representation of densities of stable laws by special functions. Theory Probab Appl 1994;39(2):354–62. http://dx.doi.org/10.1137/1139025.